Contemporary Mathematics
https://ojs.wiserpub.com/index.php/CM/

Research Article

Fluctuating Free Convection Flow of Casson Dusty Fluid in an Inclined Microchannel Under Wall Shear Stress and an Inclined Magnetic Field

Dolat Khan[1,2*], Gohar Ali[3], Zeeshan Ali[4], Dragan Pamucar[5], Subhan Ullah[6]

[1] Department of Mathematics, Saveetha School of Engineering, SIMATS, Saveetha University, Chennai, Tamil Nadu, 602105, India
[2] Faculty of Science, King Mongkut's University of Technology Thonburi (KMUTT), 126 Pracha Uthit Rd., Bang Mod, Thung Khru, Bangkok, 10140, Thailand
[3] Department of Mathematics, City University of Science & Information Technology, Peshawar, KPK, Pakistan
[4] Department of Information Management, National Yunlin University of Science and Technology, Douliu, Yunlin, Taiwan ROC
[5] Széchenyi István University, Győr, Hungary
[6] Department of Mathematics, University of Malakand, Chakdara, 18800, Pakistan
E-mail: dolat.khan@gmail.com

Received: 24 July 2025; **Revised:** 19 August 2025; **Accepted:** 26 August 2025

Abstract: This study examines the unsteady free convection flow of Casson dusty fluid within an inclined microchannel under the influence of wall shear stress and an inclined magnetic field. The fluid is assumed to contain uniformly dispersed electrically conductive dust particles, and heat is applied via Newtonian heating at one boundary. The governing partial differential equations representing the motion of both fluid and dust phases are derived and solved using the Poincaré-Lighthill Perturbation Technique (PLPT). Key physical parameters such as the Casson fluid parameter, Grashof number, magnetic field inclination, radiation, and dusty fluid interaction parameter are varied to analyze their effect on velocity and temperature profiles. Results reveal that increasing the Casson parameter reduces fluid velocity, while higher Grashof numbers and radiation levels enhance it. The magnetic field generates Lorentz forces that oppose the motion, thereby reducing both fluid and dust particle velocities. The inclined magnetic field and Newtonian heating significantly influence thermal and flow behavior. These findings have practical implications in microfluidics, industrial coatings, biomedical flows, and heat management systems, where controlling dusty fluid dynamics under external fields is crucial.

***Keywords*:** Casson fluid, dust particles, Newtonian heating, wall shear stress, inclined magnetic field, inclined parallel plate

MSC: 76A02, 76D05, 76W05

Highlights:

• A novel configuration of Casson dusty fluid flow is analyzed through an inclined microchannel under the effects of wall shear stress and Newtonian heating.

• The impact of an *inclined magnetic field*, rather than the traditionally considered perpendicular or parallel field, is studied in detail.

• Dust particles are uniformly dispersed in the Casson fluid, and their dynamics are modeled using advanced perturbation methods.

DOI: https://doi.org/10.37256/cm.6620257975

• The Poincaré-Lighthill Perturbation Technique (PLPT) is applied to obtain semi-analytical solutions, offering a unique solution framework.

• The study offers new insights into how simultaneous magnetic, thermal, and mechanical effects govern dusty fluid behavior—relevant to engineering systems like reactors, heat exchangers, and microfluidics.

Abbreviation

WSS	Wall Shear Stress
NHC	Newtonian Heating Condition
MHD	Magnetohydrodynamics
PLPT	Poincaré-Lighthill Perturbation Technique
ICs	Initial Conditions
BCs	Boundary Conditions
Nu	Nusselt Number
CFD	Computational Fluid Dynamics
Cu	Copper
Al_2O_3	Aluminum Oxide
TiO_2	Titanium Dioxide

Nomenclature

Symbol	Description	SI unit
u	Fluid velocity	$m{\cdot}s^{-1}$
v	Dust particle velocity	$m{\cdot}s^{-1}$
ρ	Fluid density	$kg{\cdot}m^{-3}$
μ	Dynamic viscosity of fluid	Pa·s
τ_w	Wall shear stress	$N{\cdot}m^{-2}$
g	Acceleration due to gravity	$m{\cdot}s^{-2}$
α	Inclination angle	rad (or degrees °)
B_0	Magnetic field strength	T (Tesla)
σ	Electrical conductivity	$S{\cdot}m^{-1}$
k	Thermal conductivity	$W{\cdot}m^{-1}{\cdot}K^{-1}$
T	Temperature	K
ν	Kinematic viscosity	$m^2{\cdot}s^{-1}$
Gr	Grashof number	(dimensionless)
M	Magnetic parameter	(dimensionless)
R	Radiation parameter	(dimensionless)
β	Casson fluid parameter	(dimensionless)
Nu	Nusselt number	(dimensionless)
CfC_f	Skin friction coefficient	(dimensionless)
q	Heat flux	$W{\cdot}m^{-2}$
y	Distance perpendicular to the plates	m
t	Time	s

1. Introduction

When two separate aggregating phases of the same substance or two different substances interact, a two-phase flow develops. The mass transfer of liquid-liquid solvents and the flow of oil-water mixtures in cylinders are two examples of uses for this type of flow. Stirring contractors, pipeline contractors, packet columns, and pulsed columns are some of the instruments utilized in solvent extraction. Furthermore, bubbles, rain, sea waves, foam, cryopreservation, slush, and oil slicks are depicted in two-phase flow paintings. The heating and power systems aboard rockets, as well as fluid management and storage, are important uses of two-phase flows in microgravity (e.g., condensers, evaporators, piping systems). To illustrate, Santosh et al. [1] investigated how fluid flow and particle mobility were affected by partial slip and heat radiation. Examining the Rheological Characteristics of an Upper Convected Maxwell Fluid on a Permeable Stretched Sheet: Insights from the Comparative Study by Abdelsalam et al. [2]. Wei et al. [3] explore the transformation system for displaying the physical characteristics of gas-liquid two-phase flow. In many industrial processes, like the production of paper, the extrusion of metals and polymers, etc., process design professionals are concerned with the effective transmission of heat and mass. Non-Newtonian fluids are also common in industry. Thus, an attempt is made to explain the unsteady Magnetohydrodynamics (MHD) flow of a Casson fluid across a semi-infinite vertical plate with thermal diffusion, radiation, and heat absorption effects. Slip boundary restrictions are also taken into consideration for this investigation. Also the Analysis of semi-infinite vertical plate is passed by an unstable MHD Casson fluid flow with thermal diffusion by Reddy et al. [4]. By using non-uniform flow surfaces, Silu et al. [5] investigated how dust particles and magnetic fields influenced the transport of heat and velocity in fluids.

Heat transmission in non-Newtonian fluids like dust particles was examined by Attia et al. [6]. Theoretical Investigation of heat and mass transfer depictions in Nanofluids Proximate to a Solid Domain by Li et al. [7]. In the realm of materials science, Abdelsalam et al. [8] present an innovative exploration into the biomimetic enhancement of nanoparticles on a robust substrate, strategically maneuvering through viscous slime. Their physical approach sheds light on the intricate interplay between nanomaterials and challenging environments, paving the way for novel applications. Concurrently, Bhatti et al. [9] contribute to the landscape of renewable energy engineering, elucidating the pivotal role of nanofluids. Through a comprehensive analysis, they unveil the potential of nanofluids to revolutionize energy harvesting and utilization, presenting a compelling case for their integration into sustainable engineering practices. These studies collectively underscore the transformative impact of interdisciplinary research on materials and energy science, pushing the boundaries of innovation for a more sustainable future. In order to understand how a magnetic field and thermal radiation affect the transfer of heat in a dusty viscoelastic fluid that conducts electricity between two stiff, non-conducting surfaces, Ali et al. [10] looked at the influences of both. The magnetic field had an astonishing influence on the flow, which in turn had an impact on the shear stress, as they had observed. Khan et al. [11] employed the Light Hill technique to establish the analytical solution for the influence of two-phase fluctuation flow of dusty fluid with wall shear stresses. In a similar research, Khan et al. [12] investigated elastic dusty fluid in an inclined channel while absorbing heat and discovering a scientific consequence of wall shear stress.

In many industrial polymers, shear thinning and thickening are frequent occurrences, and the viscosity of such a fluid relies on the rate of shear. It is typical for fluids with a shear rate dependent on viscosity to exhibit rheological behavior under yield stress. Common examples of these materials are ketchup, nail paint, polymer solutions, hair gel, and blood. Casson fluid is a fluid that thins under shear and is one of the pseudoplastic fluids. Shear-thinning fluids have viscosities that are higher at low shear rates and decrease at high shear rates when compared to Newtonian fluids. Rheological models were developed for these materials by Casson [13]. Numerous elements of flow and heat transmission for these resources have been researched up until recently. But in this section, we focus on the most important research. With the use of an illustration of a porous surface exposed to thermal radiation, Pramanik [14] looked into the transport of heat over an exponentially moving sheet in a Casson fluid flow. Muradiation [15] looked at the Casson fluid's erratic flow across a moving sheet. Bhattacharyya et al. [16] looked into the magnetohydrodynamic Casson fluid's stagnation point flow for heat transmission to exposed thermal radiations. The materials mentioned above give a clear illustration of the major effect of the yield stress on heat exchange and flows. Dash et al. [17] tested the Casson fluid flow in a cylinder formed of a uniform and porous material. Imran et al. [18] successfully solved the free convection circulation of Casson fluid

along a vertically vibrating plate using the Laplace transform. The accurate solutions to the Casson of boundary layer flows through a porous stretched sheet were given, according to Bhattacharyya et al. [19]. Hussnan et al. [20] solved the boundary layer unsteady of Casson fluid with heat exchange and Newtonian heating through an oscillating vertical plate using the Laplace transform method. For the free convection MHD flow of Casson fluid through a porous medium across an oscillating vertical plate, Khalid et al. [21] accurately solved the problem. Using a range of boundary conditions and analytical methodologies, several academics have quantitatively computed or examined findings from Casson fluids [22]. Uygun and Turkyilmazoglu [23] investigate the MHD non-Newtonian Bingham fluid flow and heat transfer over a rotating disk regulated by a uniform radial electric field. In another study, Abbas et al. [24] conducted a thermodynamic analysis of a radiative, chemically reactive Sutterby nanofluid flow influenced by induced MHD over a nonlinearly stretching cylindrical surface. Furthermore, Abbas et al. [25] carried out a theoretical investigation into the flow dynamics of a non-Newtonian micropolar nanofluid across an exponentially stretching surface, incorporating the effects of free stream velocity to better understand fluid behavior in engineering applications. Also, Ali et al. [26] of the Stokes second point for the Casson fluid between the outer side mixes the Fourier sine and cosine transforms with the Laplace transform to get the exact solution. The impacts of magnetism, chemical processes, heat production, and Newtonian heat are studied in the Casson fluid mixed convection across a moving vertically plate embedded within a porous medium. Khan et al. [27].

Numerous empirical and theoretical studies on MHD flow have been conducted in a variety of physical, commercial, and geophysical disciplines. Particularly, the MHD flows related to heat transfer have attracted a lot of interest up to this point. Applications of MHD flows may be found in a wide range of industrial domains, such as cooling of electric propulsion for space exploration, microelectronic devices, such as cooling nuclear reactors, crystal formation in liquids, electronic packaging, etc. According to the author's understanding, MHD flow analysis of a stretched wall was originally performed by Pavlov [28]. He discussed the analysis while a uniform magnetic field was present and came up with the precise analytical answer made some significant contributions to MHD flow with heat transmission [29]. Turkyilmazoglu et al. [30] have contributed extensively to the study of MHD flows under different physical settings. In one investigation, they analyzed viscous flow through a porous-walled pipe and reported the asymptotic effects of MHD forces on the velocity field. In another study, the same author examined heat transfer characteristics in MHD fluid flow over a rotating disk, highlighting the role of varying Prandtl numbers under the influence of a uniform radial electric field [31]. More recently, Turkyilmazoglu and Alotaibi [32] explored MHD Stokes flow inside a cavity driven by parallel moving lids, providing new insights into how electromagnetic forces alter the boundary-layer structures and flow stability. Collectively, these works establish a strong foundation for understanding Lorentz-force-induced damping in complex geometries, which is directly relevant to the present problem. Chhabra et al. [33] conducted a study employing the boundary element method to examine viscous fluid flow within a microchannel featuring out-of-phase slip patterns, subjected to an inclined magnetic field. In another investigation, Chhabra et al. [34] explored the influence of both magnetic fields and hydrodynamic slip conditions on electro-osmotic Brinkman flow in microchannels with spatially varying zeta potentials. Vimala et al. [35] highlighted the significance of the magnetic Reynolds number in enhancing heat transfer during MHD forced convection processes. Sekha et al. [36] analyzed the steady-state viscous flow behavior around a circular cylinder under the impact of an aligned magnetic field. Rashidi et al. [37] performed a computational investigation of the problem of the MHD flow of a fluid approaches a revolving disc with variable properties. Furthermore, they examined how the formation of heat, entropy, and momentum was affected by the electromagnetic contact number, slip component, and comparative temperature gradient. Pal and Mondal [38] investigated MHD convective heating along a wedge with heat transfer and temperature-dependent viscosity. In MHD extended non-Darcy mixed convection flow component dispersion, Pal and Mondal [39] discovered the effects of heat viscous and changing heat capacity. An equivalent integral transformation was utilized in Haq et al.'s [40].

The significance of Newtonian heating has been extensively studied in the literature. According to Newton's law of cooling, the rate at which a body loses heat is directly proportional to the temperature difference between the body and its surroundings. Regarding heat transmission around fins, heat exchanger design, and related heat transfer, Newtonian heating is widely used in the petroleum, solar, and building heating and cooling sectors. Due to its many application fields in wire coatings and spinning natural polymers, the challenge of convection and radiation in cylinders is of interest to scientists all over the world. Merkin [41] outlined four different routes by which heat may go from the surface to the

liquid. So keep it in mind. A second-grade fluid travelling in a vertical channel generated by Newtonian forces was studied by Mabood et al. [42]. Moreover, he provided illustrative simulations of these findings in the mixed convection inclination magnetic field. With regard to the movement of Casson fluid while being heated by Newtonian forces and sliding down a stretchable linear cylinder, Murthy et al. [43] make some significant discoveries. These investigations imply that the fluid's ability to convey heat and temperature is enhanced by greater Newtonian heating values Khan et al. [44] utilized second law modeling to investigate the effects of Newtonian heating on the boundary layer flow and heat transfer of a viscoelastic dusty fluid within a moving frame. In a separate study, Khan et al. [45] explored the mixed convection boundary layer flow of a viscoelastic dusty fluid combined with Newtonian heating in a rotating frame.

In prior research, the authors examined various types of dusty fluids, analyzing their properties through energy and heat transfer equations, with particular attention to some fluids that exhibit electrical conductivity. These studies laid the groundwork for understanding the complex interactions in dusty fluid dynamics [46–48].

The present study explores the dynamics of dusty Casson fluid flow, considering the interplay of inclined magnetic fields, wall shear stress, and Newtonian heating in an inclined microchannel. Dusty Casson fluids, which display yield stress and shear-thinning behavior, are highly relevant in industries where suspensions such as blood, polymers, inks, or slurries flow through confined geometries. The inclusion of dust particles adds a second phase that mimics real-world complexities, such as sediment transport or contaminant dispersal. The inclined magnetic field introduces Lorentz forces that influence flow control in electromagnetic pumps or filtration systems. To analyze this multifaceted problem, the PLPT is applied to obtain analytical solutions. The resulting velocity and temperature profiles are examined graphically to elucidate how magnetic, thermal, and particulate effects modulate the Casson fluid flow, offering insights with practical significance for engineering and biomedical applications.

2. Formulation of the problem

To develop a physically consistent and mathematically tractable model, the following assumptions were made:

1. Unsteady, unidirectional, and incompressible flow:

The flow is considered unsteady to reflect realistic time-dependent variations in velocity and temperature commonly observed in natural and industrial convection scenarios. The unidirectional assumption simplifies the flow field, allowing the velocity to vary only in one direction (along the y-axis), which is appropriate for flow between two infinite parallel plates. Incompressibility is assumed since most liquid-phase flows at low Mach numbers exhibit negligible density changes.

2. Dusty Casson fluid with spherical particles:

The Casson model is chosen because it accurately represents non-Newtonian fluids with yield stress behavior, which is relevant to industrial fluids like paints, blood, and polymers. The dust particles are assumed to be spherical and uniformly distributed to simplify the momentum exchange between the base fluid and the particulate phase. This assumption is standard in two-phase flow modeling, ensuring tractable mathematical expressions.

3. Electrically conducting dust particles in a magnetic field:

The inclusion of electrical conductivity enables the fluid-particle interaction with the externally applied inclined magnetic field, which induces Lorentz forces. This consideration is critical for MHD effects. The inclined orientation of the magnetic field is essential to reflect more realistic industrial settings where magnetic fields are rarely aligned perfectly with coordinate axes.

4. Newtonian heating condition on the left plate:

This condition is introduced to model convective boundary heating, where heat transfer depends on the temperature difference between the surface and ambient fluid. It is more general and physically meaningful than constant wall temperature, especially for applications in thermal coating and cooling technologies.

5. Wall Shear Stress (WSS) and free stream motion:

The left plate is subjected to wall shear stress, while the right plate moves with a constant free-stream velocity. This boundary setup mimics Couette-type flow driven by wall motion and shear, which is significant for understanding

lubrication and coating processes. The imposed shear stress is also crucial in modifying the momentum exchange near the wall, affecting both fluid and dust particle velocities, as present in Figure 1.

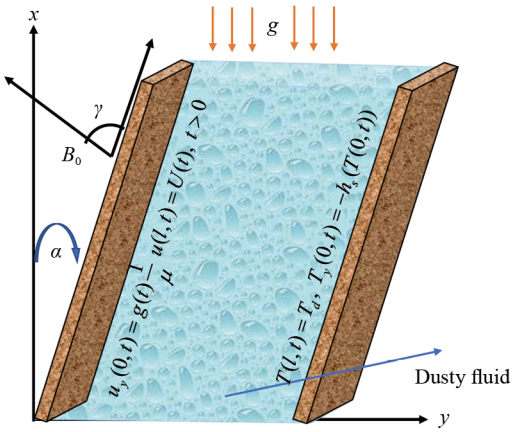

Figure 1. Geometry of the flow

The inflow and outflow equation as [10–13, 18, 44, 45]:

$$\Delta.\vec{V} = 0 \tag{1}$$

The momentum equation of the fluid flow [10–13, 18, 44, 45, 49, 50]:

$$u_t = \upsilon\left(1+\frac{1}{\beta}\right)u_{yy} + \frac{K_0 N_0}{\rho}(v-u) - \frac{\sigma B_0^2 u}{\rho}\sin(\gamma) + g\beta_T\,(T-T_d)\cos(\alpha) \tag{2}$$

The energy equation of the fluid as [10–13, 18, 44, 45]:

$$\rho c_p T_t = kT_{yy} - (q_r)_y \tag{3}$$

The momentum equation of the dusty fluid flow [10–13, 18, 44, 45]:

$$mv_t = K_0(u-v) \tag{4}$$

Where,

$$-(q_r)_y = 4\alpha_0\,(T-T_d) \tag{5}$$

The Initial Conditions (ICs) and Boundary Conditions (BCs) are [10–13, 18, 44, 45]:

$$\left.\begin{aligned} u_y(0,t) = g(t)\frac{1}{\mu}u(l,t) = U(t), \quad t>0 \\ T(l,t) = T_d, \quad T_y(0,t) = -h_s(T(0,t)) \end{aligned}\right\} \tag{6}$$

The dimensionsless variables listed below are employed.

$$y^* = \frac{y}{d},\ u^* = \frac{u}{u_0},\ t^* = \frac{u_0 t}{d},\ \theta^* = \frac{T-T_d}{T_\omega - T_d},\ v^* = \frac{v}{u_0} \tag{7}$$

The (*) symbol has been disregarded for simplicity. Eqs. (1), (2), (3), and (4) are transformed to:

$$u_t = \beta_1 u_{yy} + K(v-u) - Mu\sin(\gamma) + Gr\cos(\alpha)\theta \tag{8}$$

$$Pe\theta_t = \theta_{yy} + \Re^2\theta \tag{9}$$

$$v_t = P_m u - P_m v \tag{10}$$

with dimensionless BCs are:

$$\left.\begin{aligned} u_y(0,t) = g(t), \quad u(1,t) = 1 + \frac{\varepsilon}{2}\left(e^{i\omega t} + e^{i\omega t}\right) \\ \theta(1,t) = 0, \quad \theta_y(0,t) = -1 - \theta(0,t) \end{aligned}\right\} \tag{11}$$

Where,

$$M = \frac{\sigma B_0^2 d^2}{\rho\upsilon}, \quad K = \frac{K_0 N_0 d^2}{\rho\upsilon}, \quad Gr = \frac{g\beta_T d^2\left(T_\omega - T_\infty\right)}{u_0\upsilon}$$

$$Pe = \frac{\rho c_p u_0 d}{k}, \quad P_m = \frac{K_0 d}{m.u_0}, \quad \beta_1 = \left(1 + \frac{1}{\beta}\right), \quad \Re^2 = \frac{4\alpha_0^2 d^2}{k}$$

Let's suppose the following outcome to estimate the dust particles' velocity:

$$v(y,t) = v_0(y)e^{i\omega t} + O(\varepsilon) \tag{12}$$

When we inserted Eq. (12) into Eq. (10), we can get:

$$(i\omega + P_m)\, v(y,t) = P_m u(y,t) \tag{13}$$

Using the following assumption, let's determine the energy.

$$\theta(y,t) = \theta_0(y) + \theta_1(y)\varepsilon e^{i\omega t} + O\left(\varepsilon^2\right) \tag{14}$$

When Eq. (14) was inserted into Eq. (8), we received,

$$\theta(y,t) = \sinh(\Re - \Re.y).(\Re.\cosh(\Re) + \sinh(\Re))^{-1} \tag{15}$$

By using Eqs. (13) and (15) in Eq. (7), we get;

$$u_t = \beta_1 u_{yy} + K\left(\left(\frac{P_m}{i\omega + P_m}\right) - 1 - M.\sin(\gamma)\right)$$

$$+ Gr\cos(\alpha)\left(\sinh(\Re - \Re.y).(\Re.\cosh(\Re) + \sinh(\Re))^{-1}\right) \tag{16}$$

$$u_t = \beta_1 u_{yy} + c_0 u + Gr\cos(\alpha)\left(\sinh(\Re - \Re.y).(\Re.\cosh(\Re) + \sinh(\Re))^{-1}\right) \tag{17}$$

Where, $c_0 = \dfrac{K(M.\sin(\gamma)+1)(i\omega + P_m) - Pm}{i\omega + P_m}$.

3. Problem solution

The Light Hill Technique, [44] can be used to get the solution to Eq. (17).

$$u(y,t) = \xi_0(y) + \frac{\varepsilon}{2}\xi_2(y)e^{-i\omega t} + \frac{\varepsilon}{2}\left(\xi_1(y)e^{i\omega t}\right) \tag{18}$$

Incorporating Eq. (18) in Eq. (17) as the values shown below.

$$\xi_0(y) = \left\{ \begin{array}{l} \left(\left(1 - \dfrac{\sinh\left(\sqrt{c_1}\right)}{\sqrt{c_1}}(g(t) - R_1)\right)\dfrac{\cosh\left(\sqrt{c_1}.y\right)}{\cosh\left(\sqrt{c_1}\right)}\right) + \left((g(t) - R_1)\dfrac{\sinh\left(\sqrt{c_1}.y\right)}{\left(\sqrt{c_1}\right)}\right) \\ \\ +H\left(\sinh(\Re - \Re.y)(\Re.\cosh(\Re) + \sinh(\Re))^{-1}\right) \end{array} \right\} \tag{19}$$

Where, $H = \dfrac{.Gr.\cos(\alpha)}{c_0}$, $R_1 = \dfrac{\Re.G.\cosh(\Re)}{\Re\cosh(\Re) + \sinh(\Re)}$, $c_1 = \dfrac{c_0}{\beta_1}$

$$\xi_1(y) = \frac{\cosh\left(y.\sqrt{c_2}\right)}{\cosh\left(\sqrt{c_2}\right)} \tag{20}$$

$$\xi_2(y) = \frac{\cosh\left(y.\sqrt{c_3}\right)}{\cosh\left(\sqrt{c_3}\right)} \tag{21}$$

Where, $c_2 = \dfrac{c_0 - i\omega}{\beta_1}$, $c_3 = \dfrac{c_0 + i\omega}{\beta_1}$.

Finally, when we combine Eqs. (19), (20), and (21) in Eq. (18), we get the conclusion shown in Eq. (22).

$$u(y,t) = \left\{ \begin{array}{l} \left(\left(1 - \dfrac{\sinh\left(\sqrt{c_1}\right)}{\sqrt{c_1}}\left(g(t) - R_1\right)\right)\dfrac{\cosh\left(\sqrt{c_1}.y\right)}{\cosh\left(\sqrt{c_1}\right)}\right) + \left(\left(g(t) - R_1\right)\dfrac{\sinh\left(\sqrt{c_1}.y\right)}{\left(\sqrt{c_1}\right)}\right) \\ + \left\{H\sinh(\Re - \Re.y)(\Re.\cosh(\Re) + \sinh(\Re))^{-1}\right\} \\ + \dfrac{\varepsilon}{2}\cosh\left(y.\sqrt{c_2}\right)\left(\dfrac{1}{\cosh\left(\sqrt{c_2}\right)}\right)e^{i\omega t} + \dfrac{\varepsilon}{2}\left(\dfrac{\cosh\left(y.\sqrt{c_3}\right)}{\cosh\left(\sqrt{c_3}\right)}\right)e^{-i\omega t} \end{array} \right\}. \tag{22}$$

4. Nusselt number and skin friction

The related from Ali et al. [51] derives skin friction expressions and Nusselt number expressions from Equations (15) and (22) respectively.

$$Nu = -\left.\frac{\partial T(y,t)}{\partial y}\right|_{y=0} \tag{23}$$

$$Cf = \left.\frac{\beta_1 \partial u(y,t)}{\partial y}\right|_{y=0}. \tag{24}$$

5. Results and discussion

This study investigates the behavior of Casson dusty fluid under the influence of an inclined magnetic field and fluctuating free convection flow across an inclined parallel plate, considering the effects of wall strains and Newtonian heating. The figures below illustrate the differing velocities of fluid and dust particles, generated using the Mathcad-15 program.

Figure 2a and 2b depict the impact of the Grashof number on the velocity profiles of fluid and dust particles. These graphs show a clear correlation between the velocities of the base fluid and dust particles, with both increasing as the Grashof number rises. The Grashof number, representing the ratio of buoyancy to drag forces, indicates that higher buoyancy forces and lower viscosity lead to greater velocities.

Figure 3a and 3b illustrate the role of Lorentz forces, represented by magnetic parameters, in affecting fluid dynamics and internal resistance. This magnetic influence on fluid and dust particle velocities within the boundary layer serves as a crucial control mechanism with significant industrial and engineering applications. For instance, in environmental engineering, magnetic manipulation is essential for advanced filtration systems, allowing for targeted pollutant separation

from water or air. In manufacturing, precise control of fluid flows enhances machinery cooling processes and the handling of molten materials, ensuring safety and efficiency. In aerospace and automotive engineering, regulating coolant flows via magnetic fields optimizes engine performance and longevity. Thus, understanding and utilizing Lorentz forces can lead to innovative solutions across various industries, significantly improving process optimization and product development.

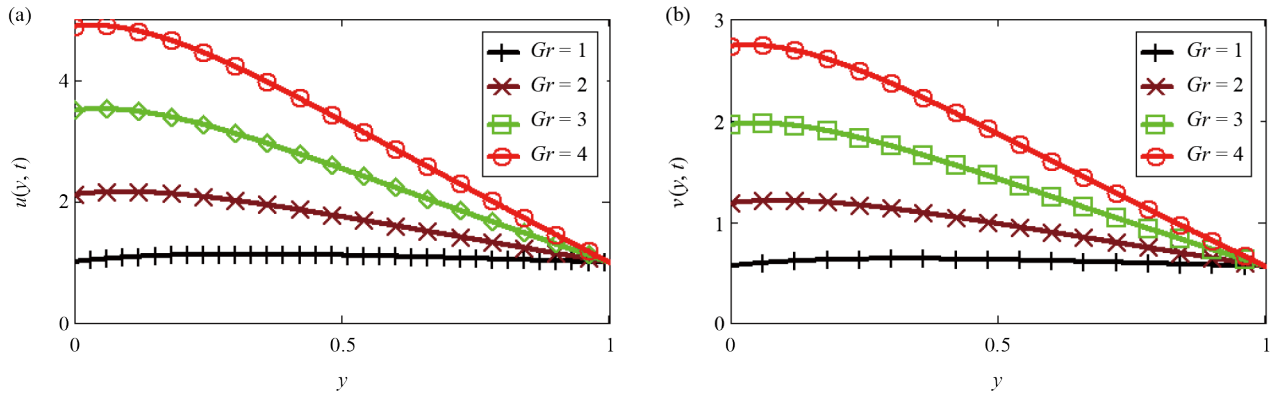

Figure 2. Effect of Gr on the velocity of the fluid and dust particles

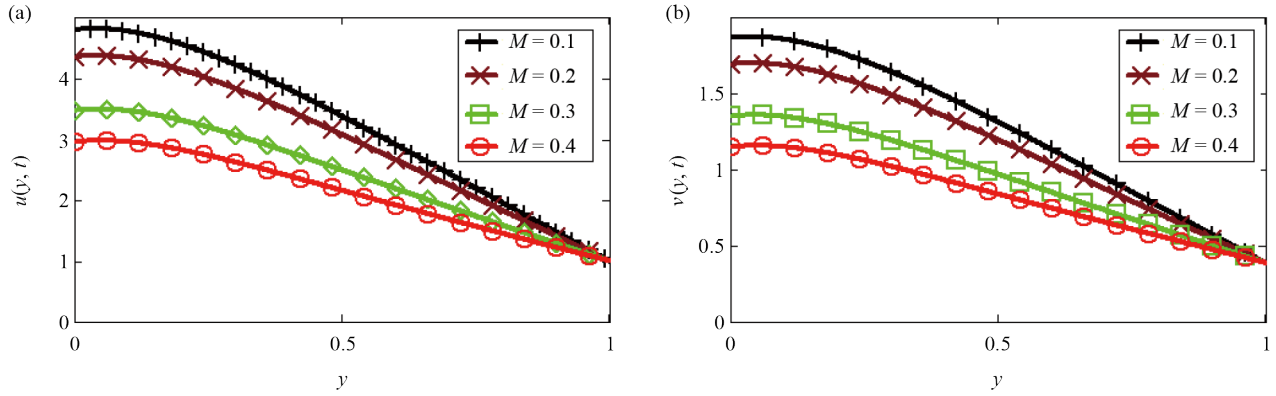

Figure 3. Effect of M on the velocity of the fluid and dust particles

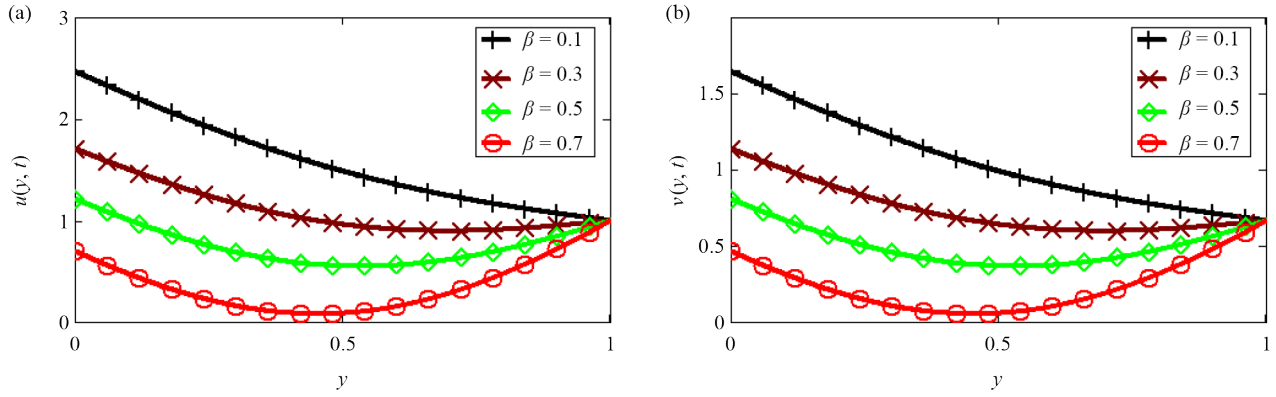

Figure 4. Effect of β on the velocity of the fluid and dust particles

Figure 4a and 4b illustrate the impact of the Casson fluid parameter on fluid dynamics, revealing a decrease in both fluid velocities and boundary layer thickness with an increase in the Casson parameter. This correlation suggests that a higher Casson parameter enhances fluid viscosity, leading to a thinner boundary layer. The study further explores how this parameter influences dust particle density within the fluid. In practical applications, such as in the coating industry, understanding the Casson fluid parameter's effect allows for the precise control of paint or coating thickness, ensuring uniform application and optimal material properties. Similarly, in environmental engineering, manipulating the Casson parameter can enhance sedimentation processes, improving the efficiency of water treatment by facilitating the settlement of particulate matter.

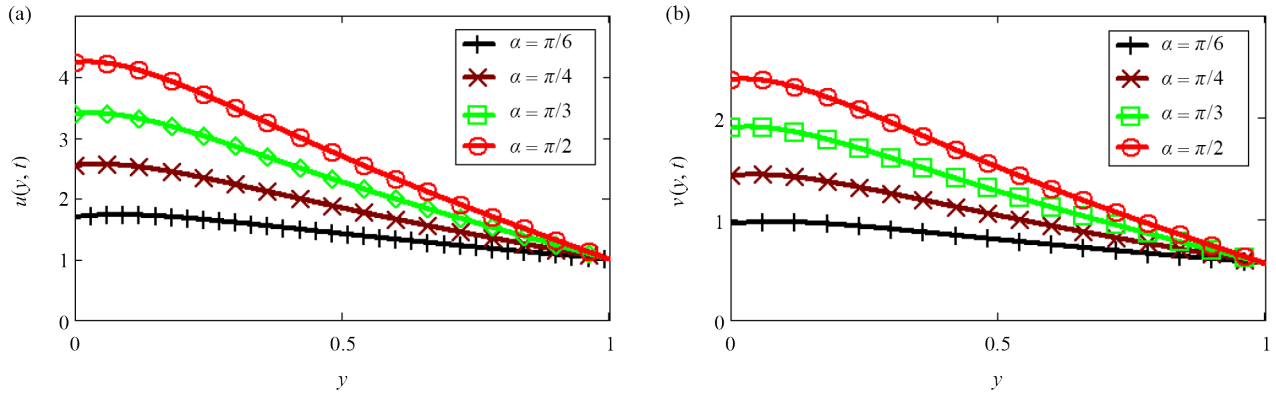

Figure 5. Effect of α on the velocity of the fluid and dust particles

Plotted are several values of the angle of inclination α in Figure 5a and 5b. It is discovered that the velocity of the fluid and dust particles is higher than at $\alpha = \frac{\pi}{2}$, and relative to $\alpha = \frac{\pi}{6}$, $\alpha = \frac{\pi}{3}$, and $\alpha = \frac{\pi}{4}$. According to the read section, the velocity approaches one at the right plate and reaches its maximum at the left plate.

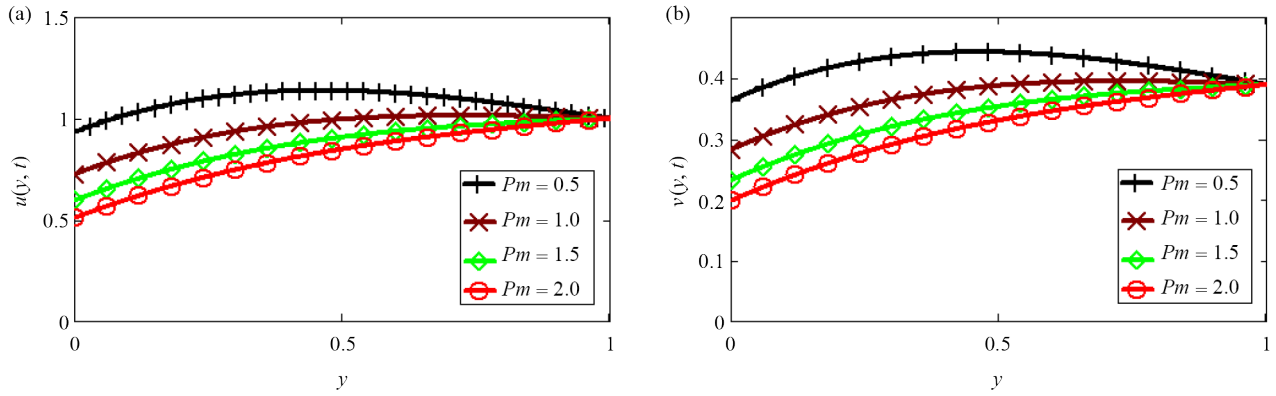

Figure 6. Effect of P_m on the velocity of the fluid and dust particles

Figure 6a and 6b show the effects of P_m on the velocities of dust particles and fluids, respectively. As P_m is inversely proportional to the mass of the dust particle, an increase in P_m causes the mass of the dust particle to drop, improving the velocity of the dust particle and fluid.

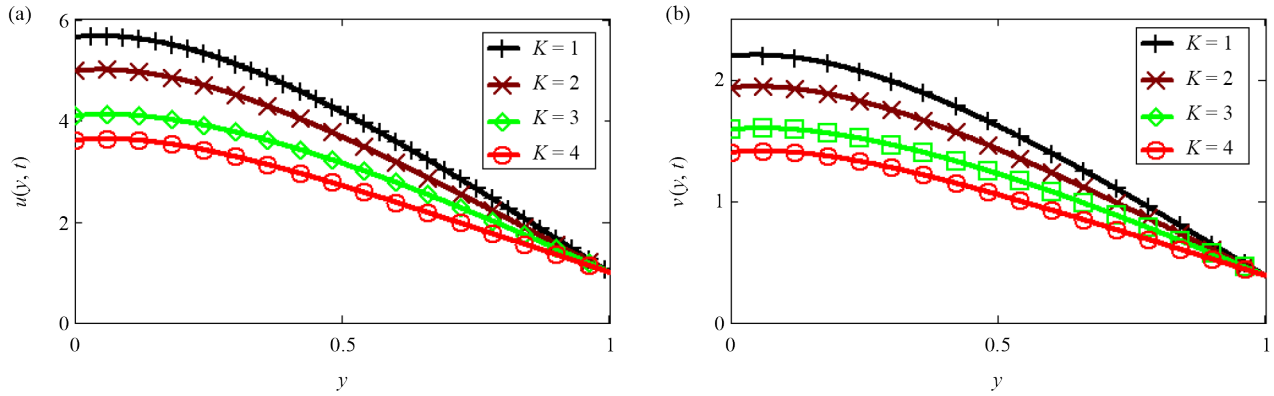

Figure 7. Effect of K on the velocity of the fluid and dust particles

Figure 7a and 7b illustrate how the dusty fluid parameter affects both velocities. The graphic makes it obvious that both velocities drop as the values rise. This behaviour is accurate since it can be shown from Stocks drag formula ($K = 6\pi r\mu$), that when viscous forces grow, the flow is resisted and both velocities fall as a result.

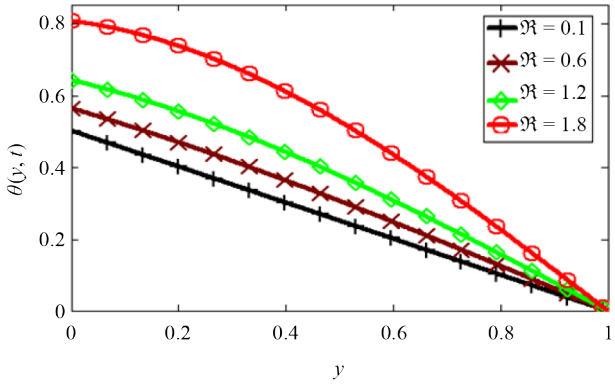

Figure 8. Effect of $\Re$ on temperature profile

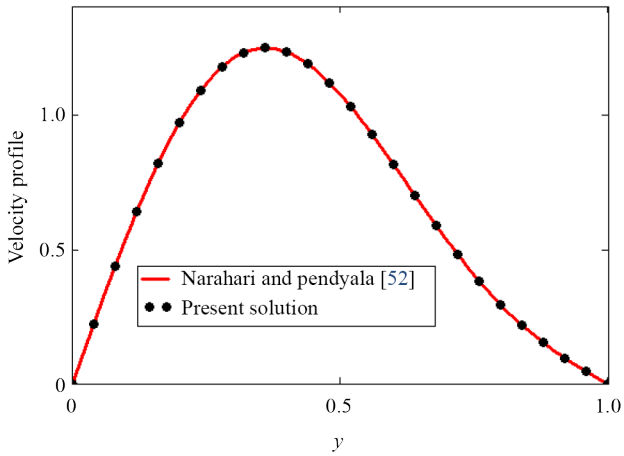

Figure 9. Comparison of the present solutions obtained in Equation (22). When $M = K = 0$, $\beta_1 = 1$, $\psi(1, t) = 0$, and $g(t) = 0$ with Narahari and Pendyala Equation (11)

Figure 8 elucidates the effect of temperature on fluid dynamics, revealing that an enhancement in the radiation parameter leads to a higher fluid temperature. This increase in temperature, because of augmented radiation, subsequently boosts the fluid's velocity. This phenomenon has significant applications, particularly in thermal management systems and energy conversion processes. For instance, in solar thermal collectors, understanding and leveraging this relationship can optimize the efficiency of converting solar energy into thermal energy, enhancing the flow rates of heat transfer fluids. Additionally, in cooling systems of power plants or electronic devices, managing the radiation parameter to control fluid temperature can improve operational efficiency and prevent overheating, ensuring the longevity and reliability of the equipment. Figure 9 is plotted to compare our solution with Narahari and Pendyala [52], showing strong agreement. Both solutions overlap exactly, demonstrating the correctness and validity of our solutions.

Table 1 reflects the influence of multiple governing parameters on the skin friction coefficient, particularly under the effects of magnetic field inclination, wall shear stress, and dusty fluid interactions. The analysis indicates that skin friction increases with the enhancement of the magnetic field parameter and the angle of inclination. This increase arises due to the intensification of Lorentz forces, which act against the fluid's motion, thereby elevating the resistance at the fluid-solid interface. Furthermore, the presence of suspended dust particles enhances the effective viscosity of the fluid, creating additional drag forces. These forces contribute to higher shear stress at the wall, which is directly measured by the skin friction coefficient. The results clearly highlight that the combined action of magnetic resistance and particulate drag strengthens the boundary interaction, which physically justifies the observed rise in skin friction values.

Table 1. Variation of Cf

β	K	$\Re$	Gr	Pe	P_m	M	α	Cf
1	0.5	10	3	2	0.5	0.5	$\pi/2$	0.774
2	0.5	10	3	2	0.5	0.5	$\pi/2$	0.931
1	0.7	10	3	2	0.5	0.5	$\pi/2$	1.006
1	0.5	12	3	2	0.5	0.5	$\pi/2$	0.810
1	0.5	10	3	3	0.5	0.5	$\pi/2$	0.974
1	0.5	10	5	2	0.5	0.5	$\pi/2$	1.119
1	0.5	10	3	2	0.6	0.5	$\pi/2$	1.922
1	0.5	10	3	2	0.5	1.0	$\pi/2$	2.209

Table 2. Variation of Nu

$\Re$	Pe	Nu
1	2	0.528
1.1	2	0.285
1	4	1.320

Table 2 presents how the Nusselt number responds to variations in thermal radiation, Newtonian heating, and fluid properties. An increasing trend in the Nusselt number is noted with higher values of the radiation parameter and Newtonian heating coefficient. This behavior is attributed to intensified thermal energy exchange at the boundary, which enhances the temperature gradient near the wall, thus promoting stronger heat transfer. Moreover, the Casson parameter, representing the non-Newtonian characteristics of the fluid, influences the thermal boundary layer. A higher Casson parameter implies increased fluid resistance to deformation, affecting both the velocity and temperature profiles. The thicker thermal boundary layer results in a steeper temperature gradient at the wall, leading to an increase in the Nusselt number. These

outcomes are consistent with the underlying thermophysical mechanisms governing heat transport in non-Newtonian, particulate-laden flows.

6. Conclusion

This study investigates the fluctuating free convection flow of a Casson dusty fluid between inclined parallel plates, under the influence of an inclined magnetic field, WSS, and Newtonian Heating Condition (NHC). Utilizing the PLPT, analytical expressions for velocity and temperature profiles were derived, and the behavior of both fluid and dust particles was analyzed.

The findings highlight that:

• An increase in the Casson parameter leads to enhanced viscosity, resulting in reduced velocities for both fluid and dust phases.

• The inclination angle and magnetic field significantly influence the velocity distribution by modifying Lorentz forces.

• Newtonian heating enhances fluid temperature, thereby increasing velocity through thermal gradients.

• The dusty fluid parameter impacts flow resistance, as stronger viscous drag forces reduce fluid motion.

6.1 *Applications and relevance*

The outcomes of this study have practical implications in fields such as:

• Microfluidics and MEMS devices, where managing two-phase dusty flows under magnetic fields are crucial.

• Biomedical engineering, for drug delivery systems and blood flow simulations involving non-Newtonian fluids like Casson-type materials.

• Thermal management systems, where an improved understanding of Newtonian heating can lead to better heat dissipation designs in electronics and reactors.

• Environmental and chemical engineering, where dust-laden flows are involved in pollutant transport or slurry handling in inclined channels.

6.2 *Demerits of the current method*

Although the PLPT provides a useful approximate analytical solution for the flow and heat transfer characteristics of dusty Casson fluids under inclined magnetic fields, it has certain limitations. The method is inherently valid only for small perturbation parameters, which restricts its applicability to cases where nonlinear effects are not dominant. Moreover, PLPT assumes idealized boundary conditions and simplified geometries, making it less accurate for highly complex or turbulent flow systems. In such scenarios, more robust numerical techniques or higher-order analytical methods may be required to capture the complete physics of the problem accurately.

6.3 *Future research directions*

To build upon this work, the following extensions are proposed:

1. Non-Parallel Plate Geometries: Investigating curved or wavy channels to understand the effect of geometry on flow behavior in industrial applications [53].

2. Nanofluid Suspensions: Replacing dust particles with hybrid nanoparticles to explore advanced heat transfer applications in thermal management systems.

3. Fractional Derivative Models: Applying fractional-order calculus to capture memory effects in viscoelastic Casson fluids for more accurate real-world modeling.

4. Three-Dimensional Simulation: Extending the study to three-dimensional domains using CFD tools to explore vortex formation and turbulence transition [54].

Data availability

The database used and analyzed during the current study are available from the corresponding author on reasonable request.

Author contribution

All authors contributed equally to the conception, analysis, and preparation of the manuscript.

Conflict of interest

The authors declare no competing financial interest.

References

[1] Santosh HB, Raju CS, Makinde OD. The flow of radiated carreau dusty fluid over an exponentially stretching sheet with partial slip at the wall. *Diffusion Foundations*. 2018; 16(2): 96-108.

[2] Abdelsalam SI, Abbas W, Megahed AM, Said AA. A comparative study on the rheological properties of upper convected Maxwell fluid along a permeable stretched sheet. *Heliyon*. 2023; 9(12): e22740. Available from: https://doi.org/10.1016/j.heliyon.2023.e22740.

[3] Wei J, Du M, Wang RN, Duan JL, Gao ZK. Symbolic transition network for characterizing the dynamics behaviors of gas-liquid two-phase flow patterns. *Physica A: Statistical Mechanics and Its Applications*. 2023; 611: 128449. Available from: https://doi.org/10.1016/j.physa.2023.128449.

[4] Reddy KV, Ramana Reddy GV, Sandhya A, Krishna YH. Numerical solution of MHD, Soret, Dufour, and thermal radiation contributions on unsteady free convection motion of Casson liquid past a semi-infinite vertical porous plate. *Heat Transfer*. 2022; 51(3): 2837-2858. Available from: https://doi.org/10.1002/htj.22452.

[5] Silu SM, Wainaina M, Kimathi M. Effects of magnetic induction on MHD boundary layer flow of dusty fluid over a stretching sheet. *Global Journal of Pure and Applied Mathematics*. 2018; 14(9): 1197-1215.

[6] Attia HA, Ewis KM. Magnetohydrodynamic flow of continuous dusty particles and non-Newtonian Darcy fluids between parallel plates. *Advances in Mechanical Engineering*. 2019; 11(6): 1-11. Available from: https://doi.org/10.1177/1687814019857349.

[7] Li S, Safdar M, Taj S, Bilal M, Ahmed S, Khan MI, et al. Generalised Lie similarity transformations for the unsteady flow and heat transfer under the influence of internal heating and thermal radiation. *Pramana*. 2023; 97(4): 203. Available from: https://doi.org/10.1007/s12043-023-02672-4.

[8] Abdelsalam SI, Zaher AZ. Biomimetic amelioration of zirconium nanoparticles on a rigid substrate over viscous slime—a physiological approach. *Applied Mathematics and Mechanics*. 2023; 44(9): 1563-1576. Available from: https://doi.org/10.1007/s10483-023-3030-7.

[9] Bhatti MM, Vafai K, Abdelsalam SI. The role of nanofluids in renewable energy engineering. *Nanomaterials*. 2023; 13(19): 2671. Available from: https://doi.org/10.3390/nano13192671.

[10] Ali F, Bilal M, Sheikh NA, Khan I, Nisar KS. Two-phase fluctuating flow of dusty viscoelastic fluid between non-conducting rigid plates with heat transfer. *IEEE Access*. 2019; 7(2): 123299-123306. Available from: https://doi.org/10.1109/ACCESS.2019.2933529.

[11] Khan D, Ali G, Kumam P, Ur Rahman A. A scientific outcome of wall shear stress on dusty viscoelastic fluid along heat absorbing in an inclined channel. *Case Studies in Thermal Engineering*. 2022; 30: 101764. Available from: https://doi.org/10.1016/j.csite.2022.101764.

[12] Khan D, Rahman AU, Ali G, Kumam P, Kaewkhao A, Khan I. The effect of wall shear stress on the two-phase fluctuating flow of dusty fluids by using the light hill technique. *Water*. 2021; 13(11): 1587. Available from: https://doi.org/10.3390/w13111587.

[13] Casson N. A flow equation for pigment-oil suspensions of the printing ink type. *Rheology of Disperse Systems*. 1959: 41(4): 413-421.
[14] Pramanik S. Casson fluid flow and heat transfer past an exponentially porous stretching surface in presence of thermal radiation. *Ain Shams Engineering Journal*. 2014; 5(1): 205-212. Available from: https://doi.org/10.1016/j.asej.2013.05.003.
[15] Mukhopadhyay S, De PR, Bhattacharyya K, Layek GC. Casson fluid flow over an unsteady stretching surface. *Ain Shams Engineering Journal*. 2013; 4(4): 933-938. Available from: https://doi.org/10.1016/j.asej.2013.04.004.
[16] Bhattacharyya K. MHD stagnation-point flow of Casson fluid and heat transfer over a stretching sheet with thermal radiation. *Journal of Thermodynamics*. 2013; 5(3): 1-9. Available from: https://doi.org/10.1155/2013/169674.
[17] Dash RK, Mehta KN, Jayaraman G. Casson fluid flow in a pipe filled with a homogeneous porous medium. *International Journal of Engineering Science*. 1996; 34(10): 1145-1156. Available from: https://doi.org/10.1016/0020-7225(96)00012-2.
[18] Imran MA, Sarwar S, Imran M. Effects of slip on free convection flow of Casson fluid over an oscillating vertical plate. *Boundary Value Problems*. 2016; 2016(1): 1-11. Available from: https://doi.org/10.1186/s13661-016-0538-2.
[19] Bhattacharyya K, Hayat T, Alsaedi A. Exact solution for boundary layer flow of Casson fluid over a permeable stretching/shrinking sheet. *ZAMM-Journal of Applied Mathematics and Mechanics*. 2014; 94(6): 522-528. Available from: https://doi.org/10.1002/zamm.201200031.
[20] Hussanan A, Salleh MZ, Khan I, Tahar RM. Unsteady heat transfer flow of a Casson fluid with Newtonian heating and thermal radiation. *Journal of Technology (Sciences & Engineering)*. 2016; 78(4-4): 1-7. Available from: https://doi.org/10.11113/jt.v78.8264.
[21] Khalid A, Khan I, Khan A, Shafie S. Unsteady MHD free convection flow of Casson fluid passed over an oscillating vertical plate embedded in a porous medium. *Engineering Science and Technology, an International Journal*. 2015; 18(3): 309-317. Available from: https://doi.org/10.1016/j.jestch.2014.12.006.
[22] Li S, Khan MI, Khan SU, Abdullaev S, Mohamed MMI, Amjad MS. Effectiveness of melting phenomenon in two phase dusty carbon nanotubes (Nanomaterials) flow of Eyring-Powell fluid: Heat transfer analysis. *Chinese Journal of Physics*. 2023; 86: 160-169. Available from: https://doi.org/10.1016/j.cjph.2023.09.013.
[23] Uygun N, Turkyilmazoglu M. MHD non-Newtonian Bingham fluid flow and heat transfer over a rotating disk regulated by a uniform radial electric field. *International Journal of Heat and Fluid Flow*. 2025; 116: 109899. Available from: https://doi.org/10.1016/j.ijheatfluidflow.2025.109899.
[24] Abbas N, Shatanawi W, Taqi AM. Thermodynamic study of radiative chemically reactive flow of induced MHD sutterby nanofluid over a nonlinear stretching cylinder. *Alexandria Engineering Journal*. 2023; 70: 179-189. Available from: https://doi.org/10.1016/j.aej.2023.02.038.
[25] Abbas N, Rehman KU, Shatanawi W, Al-Eid AA. Theoretical study of non-Newtonian micropolar nanofluid flow over an exponentially stretching surface with free stream velocity. *Advances in Mechanical Engineering*. 2022; 14(7). Available from: https://doi.org/10.1177/16878132221107790.
[26] Ali M, Haq SU, Ali F, Rahman AU, Sheikh NA. Stoke's second problem for Casson fluid between two side walls. *Nonlinear Science Letters A*. 2018; 9(2): 123-135.
[27] Khan D, Khan A, Khan I, Ali F, Tlili I. Effects of a relative magnetic field, chemical reaction, heat generation, and Newtonian heating on convection flow of Casson fluid over a moving vertical plate embedded in a porous medium. *Scientific Reports*. 2019; 9(1): 1-18. Available from: https://doi.org/10.1038/s41598-018-36243-0.
[28] Pavlov KB. Magnetohydrodynamic flow of an incompressible viscous fluid caused by deformation of a plane surface. *Magnetohydrodynamics*. 1974; 4(1): 146-147.
[29] Khan A, Ul Karim F, Khan I, Alkanhal TA, Ali F, Khan D, et al. Entropy generation in MHD conjugate flow with wall shear stress over an infinite plate: Exact analysis. *Entropy*. 2019; 21(4): 359. Available from: https://doi.org/10.3390/e21040359.
[30] Turkyilmazoglu M, Alotaibi A. On the viscous flow through a porous-walled pipe: asymptotic MHD effects. *Microfluidics and Nanofluidics*. 2025; 29(6): 33. Available from: https://doi.org/10.1007/s10404-025-02808-5.
[31] Turkyilmazoglu M. MHD fluid flow and heat transfer with varying Prandtl numbers due to a rotating disk subject to a uniform radial electric field. *Applied Thermal Engineering*. 2012; 35: 127-133. Available from: https://doi.org/10.1016/j.applthermaleng.2011.10.014.

[32] Turkyilmazoglu M, Alotaibi A. Analysis of MHD stokes fluid flow in a cavity driven by moving parallel lid(s). *Theoretical and Computational Fluid Dynamics*. 2025; 39(4): 31. Available from: https://doi.org/10.1007/s00162-025-00750-4.

[33] Chhabra V, Nishad CS, Sahni M. Boundary element method for viscous flow through out-phase slip-patterned microchannel under the influence of inclined magnetic field. *Chemical Product and Process Modeling*. 2024; 19(5): 825-846. Available from: https://doi.org/10.1515/cppm-2024-0065.

[34] Chhabra V, Nishad CS, Sahni M, Chaurasiya VK. Effect of magnetic field and hydrodynamic slippage on electro-osmotic Brinkman flow through patterned zeta potential microchannel. *Journal of Engineering Mathematics*. 2024; 148(1): 3. Available from: https://doi.org/10.1007/s10665-024-10391-x.

[35] Vimala S, Damodaran S, Sivakumar R, Sekhar TVS. The role of magnetic Reynolds number in MHD forced convection heat transfer. *Applied Mathematical Modelling*. 2016; 40(13-14): 6737-6753. Available from: https://doi.org/10.1016/j.apm.2016.02.019.

[36] Sekhar TV, Sivakumar R, Kumar H. Effect of aligned magnetic field on the steady viscous flow past a circular cylinder. *Applied Mathematical Modelling*. 2007; 31(1): 130-139. Available from: https://doi.org/10.1016/j.apm.2005.08.011.

[37] Rashidi MM, Kavyani N, Abelman S. Investigation of entropy generation in MHD and slip flow over a rotating porous disk with variable properties. *International Journal of Heat and Mass Transfer*. 2014; 70: 892-917. Available from: https://doi.org/10.1016/j.ijheatmasstransfer.2013.11.058.

[38] Pal D, Mondal H. Influence of temperature-dependent viscosity and thermal radiation on MHD forced convection over a non-isothermal wedge. *Applied Mathematics and Computation*. 2009; 212(1): 194-208. Available from: https://doi.org/10.1016/j.amc.2009.02.013.

[39] Pal D, Mondal H. Effects of temperature-dependent viscosity and variable thermal conductivity on MHD non-Darcy mixed convective diffusion of species over a stretching sheet. *Journal of the Egyptian Mathematical Society*. 2014; 22(1): 123-133. Available from: https://doi.org/10.1016/j.joems.2013.05.010.

[40] Haq SU, Ur Rahman A, Khan I, Ali F, Shah SIA. The impact of side walls on the MHD flow of a second-grade fluid through a porous medium. *Neural Computing and Applications*. 2018; 30(4): 1103-1109. Available from: https://doi.org/10.1007/s00521-016-2733-6.

[41] Merkin JH. Natural-convection boundary-layer flow on a vertical surface with Newtonian heating. *International Journal of Heat and Fluid Flow*. 1994; 15(5): 392-398. Available from: https://doi.org/10.1016/0142-727X(94)90053-1.

[42] Mabood F, Tlili I, Shafiq A. Features of inclined magnetohydrodynamics on a second-grade fluid impinging on a vertical stretching cylinder with suction and Newtonian heating. *Mathematical Methods in the Applied Sciences*. 2020; 2020(1): 1-13. Available from: https://doi.org/10.1002/mma.6489.

[43] Murthy MK, Raju CS, Nagendramma V, Shehzad SA, Chamkha AJ. Magnetohydrodynamics boundary layer slips Casson fluid flow over a dissipated stretched cylinder. *Defect and Diffusion Forum*. 2019; 393: 73-82. Available from: https://doi.org/10.4028/www.scientific.net/DDF.393.73.

[44] Khan D, Ali G, Kumam P, Rahman AU, Watthayu W, Galal AM. Free convective Couette flow analysis of viscoelastic dusty fluid along with Newtonian heating in a rotating frame. *Waves in Random and Complex Media*. 2025; 35(5): 10373-10395. Available from: https://doi.org/10.1080/17455030.2022.2112637.

[45] Khan D, Kumam P, Ur Rahman A, Ali G, Sitthithakerngkiet K, Watthayu W, et al. The outcome of Newtonian heating on Couette flow of viscoelastic dusty fluid along with the heat transfer in a rotating frame: second law analysis. *Heliyon*. 2022; 8(9): e10538. Available from: https://doi.org/10.1016/j.heliyon.2022.e10538.

[46] Rehman KU, Shatanawi W, Kasim ARM. On heat transfer in Carreau fluid flow with thermal slip: An artificial intelligence (AI) based decisions integrated with Lie symmetry. *International Journal of Heat and Fluid Flow*. 2024; 107: 109409. Available from: https://doi.org/10.1016/j.ijheatfluidflow.2024.109409.

[47] Bilal S, Ullah A, Rehman KU, Shatanawi W, Shflot AS, Malik MY. Heat transfer analysis of Carreau nanofluid flow with gyrotactic microorganisms: A comparative study. *Case Studies in Thermal Engineering*. 2024; 60: 104617. Available from: https://doi.org/10.1016/j.csite.2024.104617.

[48] Abbas N, Ul Huda N, Shatanawi W, Mustafa Z. Melting heat transfer of Maxwell-Sutterby fluid over a stretching sheet with stagnation region and induced magnetic field. *Modern Physics Letters B*. 2024; 38(15): 2450085. Available from: https://doi.org/10.1142/S0217984924500854.

[49] Chhabra V, Nishad CS, Sahni M. Effect of inclined magnetic field on stokes flow through in-phase slip-patterned microchannel using boundary element method. In: *2024 International Conference on Modeling, Simulation & Intelligent Computing (MoSICom)*. Dubai, United Arab Emirates: IEEE; 2024. p.51-56.

[50] Chhabra V, Nishad CS, Sahni M, Chaurasiya VK. Boundary element analysis for MHD Brinkman flow around circular cylinders inside a microchannel exhibiting wall roughness. *Engineering Analysis with Boundary Elements*. 2025; 176: 106235. Available from: https://doi.org/10.1016/j.enganabound.2025.106235.

[51] Ali G, Ali F, Khan A, Ganie AH, Khan I. A generalized magnetohydrodynamic two-phase free convection flow of dusty Casson fluid between parallel plates. *Case Studies in Thermal Engineering*. 2022; 29: 101657. Available from: https://doi.org/10.1016/j.csite.2021.101657.

[52] Narahari M, Pendyala R. Exact solution of the unsteady natural convective radiating gas flow in a vertical channel. *AIP Conference Proceedings*. 2013; 1557: 121-124. Available from: https://doi.org/10.1063/1.4823888.

[53] Turkyilmazoglu M. Bödewadt flow and heat transfer of dusty fluid with Navier slip. *Archives of Mechanics*. 2022; 74(2-3): 157-172. Available from: https://doi.org/10.24423/aom.3930.

[54] Turkyilmazoglu M, Alotaibi A. Fluid flow between two parallel active plates. *Physica D: Nonlinear Phenomena*. 2024; 470: 134373. Available from: https://doi.org/10.1016/j.physd.2024.134373.